J.E. Clavero · R.S.J. Sparks · H.E. Huppert
W.B. Dade

Geological constraints on the emplacement mechanism of the Parinacota debris avalanche, northern Chile

Abstract The Holocene Parinacota Volcanic Debris Avalanche (ca. 8,000 years B.P.) is located in the central Andes of northern Chile. The avalanche formed by the sector collapse of a major stratovolcano adjacent to a lake basin in a single, catastrophic event. The deposit has an estimated volume of ca. 6 km^3, a run-out of over 22 km, and covers more than 140 km^2 of the surrounding terrain. The values of the Heim coefficient (≈0.08) and the ratio $A/V^{2/3}$ (ca. 50), where A is the area covered and V the volume of the deposit, indicate high mobility of the avalanche debris in transport. Two avalanche units can be distinguished. The lower unit consists mainly of blocks of rhyodacitic lavas and domes and pyroclastic flow deposits, and glacial, fluvial and lacustrine sediments. The upper unit consists of a coarse-grained breccia with little matrix, largely composed of andesite blocks, which are angular with little or no rounding by abrasion. The avalanche displays pronounced hummocky topography, in which hummock volume and amplitude, as well as maximum block size within individual hummocks, tends to decrease with transport distance and towards the lateral margins of the avalanche deposit. Some surfaces of individual breccia blocks are covered by tens to thousands of small-scale impact marks, indicating that neighbouring blocks were vibrating and colliding without significant shearing motion. Most of the deformation and shearing was, instead, accommodated in a basal layer of wet, structureless sediments incorporated into the avalanche debris from the inundated lake basin. We propose that the ancestral Parinacota stratovolcano collapsed because of loading of underlying fluvioglacial and lacustrine sediments. The edifice disintegrated during collapse along existing fractures into large rock domains (volumes from 10 to greater than 1×10^6 m^3), which were transported with little internal deformation, and then fragmented into hummocks of breccia as they were deposited. The decrease of hummock volume with distance suggests that material that travelled further broke up and had an initial greater kinetic energy.

Keywords Debris avalanche · Hummocks · Impact marks · Northern Chile · Parinacota Volcano

J.E. Clavero (✉)
Servicio Nacional de Geología y Minería,
Av. Santa María 0104, Santiago-Chile
e-mail: jclavero@sernageomin.cl or jorgeclavero@yahoo.com
Tel.: +44-117-9545243, Fax: +44-117-9253385

J.E. Clavero · R.S.J. Sparks
Dept. of Earth Sciences, University of Bristol,
Wills Memorial Building, Queen's Road, Bristol BS8 1RJ, UK

H.E. Huppert · W.B. Dade
Institute of Theoretical Geophysics, Cambridge University,
Cambridge CB3 9EW, UK

Introduction

The Parinacota debris avalanche of Holocene age is situated in the Nevados de Payachata volcanic region (18°S) in the Central Andes Volcanic Zone of northern Chile (Figs. 1 and 2). Parinacota Volcano is located on the Chile–Bolivia border and is a large composite stratocone of Late Quaternary age. The present-day symmetrical stratocone (summit altitude 6,350 m and 20–25 km^3 in volume; Fig. 3a) is younger than the large debris avalanche, which was first described by Wörner et al. (1988). The young stratocone is built on the foundations of an earlier stratocone of approximately similar size, which pre-dates the debris avalanche, constructed in the upper Lauca sedimentary basin. We describe evidence that loading of the low-density sediments and pyroclastic deposits by the stratocone resulted in conditions that were favourable for edifice failure.

Geological observations can help to constrain emplacement mechanisms. Here we describe the Parinacota debris avalanche deposit with emphasis on morphological and textural features, including a basal layer of structureless sedimentary material and impact marks on the surfaces of blocks. The upper unit of the debris avalanche shows pronounced hummocky topography. The

Fig. 1 Satellite TM Landsat image (bands 7, 4, 1) of Nevados de Payachata area. Toreva blocks can be seen at the western foot of the volcano and many kettle hole structures in the central and medial part of the avalanche deposit are shown. The avalanche margin is shown in *dashed white curve*. Geographical areas mentioned in the text are labelled in Fig. 2. Lakes are in *black*, ice and snow in *blue* and vegetation in *green*
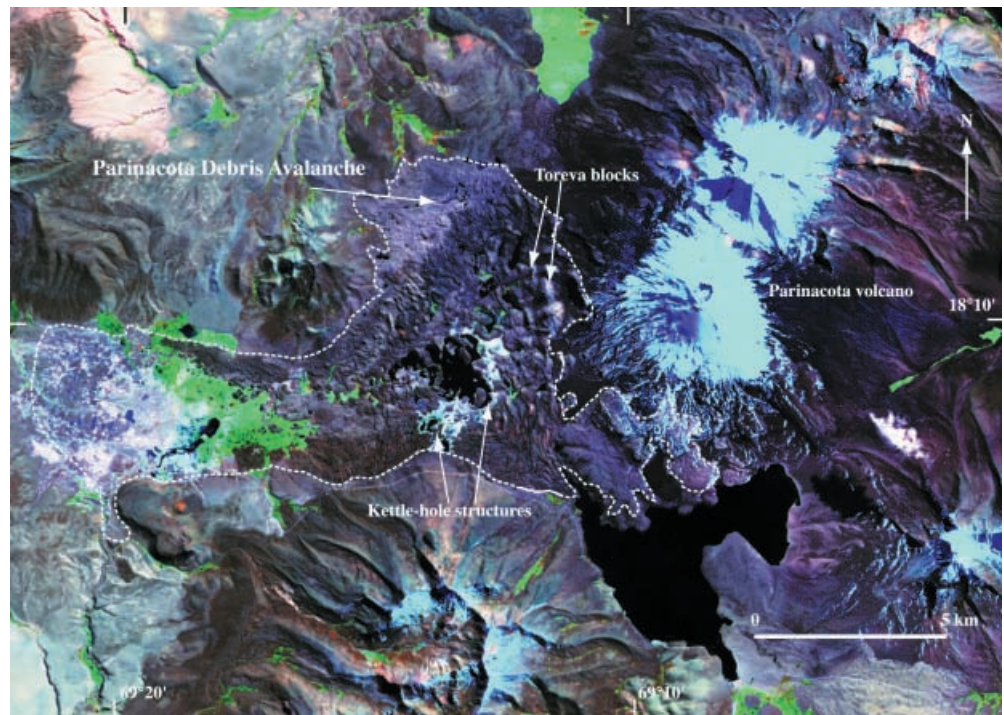

volume and height to width ratio of the hummocks decrease with distance from the proximal to distal and marginal areas. Individual hummocks consist of coarse-grained, clast-supported breccia of lava fragments. Individual clasts are angular with little signs of abrasion and there is typically little matrix in the breccias, except near the base. The lack of fine-grained matrix in the deposit makes the Parinacota avalanche an end member case because many descriptions of debris avalanche deposits indicate significant proportions of fine-grained matrix (Ui 1983; Siebert 1984; Glicken 1996). However, the basal sedimentary layer may have accommodated much of the shear during the avalanche emplacement. One striking and unexpected feature of the Parinacota avalanche deposit, which we describe here for the first time, are small-scale impact marks commonly found on the surfaces of individual clasts. They occur most prominently on weathered surfaces of andesite blocks and indicate repeated collision of neighbouring blocks with little relative movement between blocks. Accordingly, we applied a simple model for the block collisions to estimate typical impact velocities. These impact marks contrast with features in pyroclastic flow deposits, which show marked abrasion of blocks and friction marks related to tumbling and sliding of blocks in the flow (Grunewald et al. 2000). We also describe features of the deposit, such as large depressions and anomalously thin distal edges to the avalanche, which are attributed to the incorporation of ice and snow.

Several hypotheses and theoretical models have been developed to explain the long run-out of large debris avalanches. Mechanisms that may contribute to mass-flow mobility include rapid and pervasively sheared granular flow (Drake 1990; Straub 1996; Iverson 1997), in which frictional contacts may be reduced by intense acoustic energy generated by the spreading mass (Melosh 1979, 1987). In addition, solid-body friction at the base of mobile avalanche debris may be reduced because of the presence of a cushion of trapped air (Shreve 1968), molten material associated with intense heating (Goguel 1978; Erismann 1979; Legros et al. 2000), a "self-lubricating" layer of confined and intense granular flow (Campbell 1989) or the incorporation of water-saturated sediments (Crandell et al. 1984; Siebe et al. 1992). These mechanisms have been variously accommodated in the bulk treatment of avalanche debris as viscous (Hsü 1975) and Bingham flows (Eppler et al. 1987; McEwen and Malin 1989; Belousov et al. 1999; Takarada et al. 1999). Recently, Dade and Huppert (1998) advanced a model for long run-out debris avalanches for which a wide range of observations is accommodated with a constant resisting stress in the range of 10–100 kPa.

The lack of consensus among these explanations and the intriguing explanatory power of Dade and Huppert's analysis serve, in part, as motivation for our study of the Parinacota avalanche deposit. We believe that none of the commonly proposed mechanisms for debris avalanche emplacement are entirely consistent with the observations and that some models, such as rapid and pervasively sheared granular flow, cannot be invoked to account for the mobility of the Parinacota avalanche. We propose that the debris avalanche was caused by failure of the overloaded water-saturated sediments of the Upper Lauca basin, underlying the ancestral Parinacota stratovolcano. The debris avalanche formed by disintegration along existing fractures and planes of weaknesses of the

Fig. 2 Location map of the study area and distribution of the Parinacota debris avalanche deposit
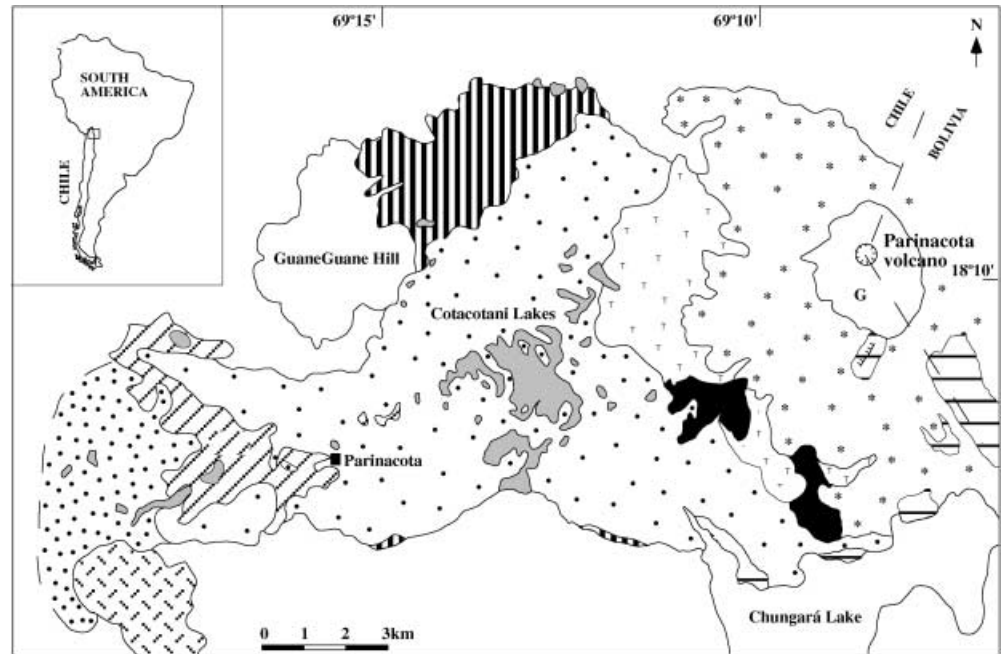
Legend

Parinacota volcano

■ Late Holocene Ajata basaltic andesite lava flows

New cone (post-avalanche): mainly andesitic lava flows, andesitic pyroclastic flow deposits and lahar deposits

Parinacota avalanche

Upper flow Unit

Area covered by continous hummocks mainly made of blocks of cpx and hb-rich andesitic lava flows

Area covered by isolated mainly conical small-scale hummocks

Lower flow Unit

Toreva blocks mainly made of rhyodacitic domes

Small size and low amplitude hummocks mainly formed by blocks of dacitic to rhyodacitic domes, lava domes and pyroclastic flow deposits

Pre-avalanche lavas and domes, dacitic to andesitic in composition

Late Quaternary Chucuyo dome

Lakes inside Parinacota avalanche

Vegetation

Glacier cap

Parinacota crater

Estimated extension of Parinacota avalanche

Avalanche scar

■ Village

stratovolcano during failure into large rock domains (with individual volumes in the range of 10 m³ to greater than 1×10⁶ m³) that were transported with little internal deformation apart from vibrations, modest internal shear in some domains and some dilation as individual domains fragmented during transport and emplacement. Spreading of the mobile debris avalanche in a fluid-like manner was mainly accommodated by the dislocation of individual domains and intense shear concentrated in a basal layer of sediment incorporated from the inundated Lauca basin. The basal layer was possibly related initially to the main décollement failure zone and, as the avalanche progressed, this probably involved water-saturated material downstream. The hummocks of breccia, which are a key characteristic of avalanche deposits, formed by disintegration of the domains as they were transported and finally deposited.

Age of the Parinacota avalanche

Francis and Wells (1988) suggested a minimum age of 13,500 years B.P. for the avalanche, based on a radiocarbon date of a peat layer at Cotacotani Lakes (Figs. 1 and 2). They interpreted the Cotacotani Lakes as being generated within the avalanche deposit and, therefore, interpreted the date as a minimum age for the collapse. Recently, Wörner et al. (2000) interpreted the age of the Parinacota avalanche as being ca. 18,000 years B.P. based on a He-exposure age obtained on a block from the deposit.

However new C¹⁴ geochronological data (Table 1) indicate that the avalanche occurred less than 8,000 years B.P. Four dates were obtained in organic-rich sediments, interbedded with tephra fallout layers at Cotacotani Lakes (Figs. 1 and 2), ranging between 12,750 and 10,650 years B.P. Two dates were obtained in palaeo-soil horizons incorporated in the debris avalanche deposit,

near Parinacota Village (8,600±170 years B.P. ca. 15 km from Parinacota Volcano, Table 1) and near Lake Chungará (7,790±100 years B.P. ca. 6 km from Parinacota Volcano, Table 1). These dates clearly give a maximum age for the avalanche, showing that the collapse of the Parinacota Volcano occurred less than 8,000 years ago. These results show that organic-rich sediments exposed in the Cotacotani Lakes area are older than the Parinacota debris avalanche. These sediments were located in the Upper Lauca basin and were buried and partly incorporated into the avalanche deposit, and are not the product of post-avalanche intra-hummock sedimentation as Francis and Wells (1988) suggested. The upper part of the Lauca basin was a fluvial and lacustrine environment prior to the deposition of the avalanche, probably dammed by glacial deposits. The present Cotacotani Lakes are interpreted as kettle hole structures within the Parinacota debris avalanche deposit as will be described later. On the other hand, the block dated by Wörner et al. (2000) probably corresponds to a lava dome previously erupted by the volcano and exposed to the atmosphere ca. 18,000 years B.P., which is almost 10,000 years prior to the collapse that generated the Parinacota avalanche.

Pre-failure environment

The Parinacota stratocone was constructed in the Upper Lauca basin (north-eastern part of the Pleistocene–Holocene Lauca basin, Kött et al. 1995). There are exposures of Lauca basin sediments beneath the avalanche and, in some cases, these sediments were incorporated in the avalanche deposit or were deformed by it. The Lauca basin sediments include fine-grained lacustrine laminated silts, cross-bedded silty to sandy deposits of fluvial or deltaic origin and sandy conglomerates. Some horizons contain reworked pumice clasts. The sandy conglomer-

Fig. 3 a Parinacota Volcano viewed from the south across Lake Chungará. The remnant of the old cone (pre-avalanche) is seen on the south-eastern side (to the *right*) with the new stratocone infilling the avalanche scar marked by the ridge at *R*. **b** Parinacota debris avalanche is seen from south-west with typical hummocky topography. Parinacota (*right peak*) and Pomerape (more distant *left peak*) stratocones can be seen. The largest hummocks, to the *left*, are proximal Toreva blocks (up to 120 m high). The avalanche margin is seen in the near foreground

Table 1 Uncalibrated radiocarbon dates of peat and palaeo-soil horizons from Parinacota Volcano area

Location and sample number	UTM co-ordinates		Material	Date (years B.P.)[a]	Stratigraphic significance
	N	E			
Cotacotani Lakes					
CAL-26B	7988845	474641	Peat	12,750±80	Age of interbedded lacustrine sediments and tephra layers buried by Parinacota avalanche
CAL-26D	7988845	474641	Peat	11,200±100	Age of interbedded lacustrine sediments and tephra layers buried by Parinacota avalanche
CAL-26E	7988845	474641	Peat	10,550±70	Age of interbedded lacustrine sediments and tephra layers buried by Parinacota avalanche
CAL-26G	7988845	474641	Peat	10,650±80	Age of interbedded lacustrine sediments and tephra layers buried by Parinacota avalanche
Near Parinacota village					
CAL-1A	7987137	471631	Palaeo-soil	8,600±170	Age of palaeo-soil horizon incorporated in Parinacota avalanche. Maximum age of Parinacota debris avalanche
Near Chungará Lake					
CAL-28B	7985791	479091	Palaeo-soil	7,790±100	Age of palaeo-soil horizon incorporated in Parinacota avalanche. Maximum age of Parinacota debris avalanche

[a] Present is 1950 A.D.

ates are particularly important in that we will later describe a basal deposit of the avalanche, which is derived from them. The conglomerates display well-developed bedding and consist of a mixture of pebbles and sand. The pebbles are largely derived from Tertiary and Quaternary volcanic rocks.

The stratocone that failed in the debris avalanche can be reconstructed from the lithology of the avalanche deposit and the remnants of the stratocone partially buried by the new post-avalanche stratocone. The reconstruction is partly based on previous work (Wörner et al. 1988) and new observations. The stratocone consisted of an older sequence of rhyodacitic lava domes and associated block-and-ash flow deposits and minor dacitic lava flows (Fig. 3a), and a younger stratocone succession predominantly composed of pyroxene andesite and hornblende andesite lava flows. The rhyodacitic block-and-ash flow deposits formed fans extending into the Lauca basin and mixed with the sediments of the basin. Remnants of the old edifice crop out in the southern and eastern flanks of the volcano (Fig. 2). They consist mainly of rhyodacitic domes and andesitic to dacitic lava flows. Their surfaces are usually weathered and show abundant thermal fractures. The remnant of the avalanche scar can be seen in the southern flank of the volcano (Fig. 3a).

General features of Parinacota debris avalanche

The geology of the area was first described by Katsui and González (1968). Wörner et al. (1988) produced a reconnaissance map of the debris avalanche and outlined a five-stage history for the Parinacota Volcano. Rocks from the first three stages defined by Wörner et al. (1988) can be identified as major constituents of the debris avalanche, with compositions ranging from basaltic andesite to rhyodacite, with andesite being the dominant rock type.

The debris avalanche deposit covers a minimum area of 140 km^2 and extends for at least 22 km (Figs. 1 and 2), with an estimated volume of 6 km^3. The volume is not well constrained because of uncertainties about pre-existing topography, lack of deep dissection, and burial of distal parts of the avalanche under younger lake sediments and vegetation. The relative run-out (the ratio of vertical fall height, assumed to have been similar to the height of the new stratocone, to run-out) known as the Heim coefficient, is estimated to be 0.08. This value falls within the range of other volcanic dry avalanches (Ui 1983). The ratio, $A/V^{2/3}$, where A is the area and V is the volume, is approximately 50, so the Parinacota avalanche mobility, in terms of this ratio, is typical of other catastrophic debris avalanches of volcanic and non-volcanic origin (Dade and Huppert 1998). The excessive travel distance (the ratio between the travelled distance and the theoretical distance, defined by Hsü 1975) is 20, falling at the more mobile end of volcanic dry avalanche values (Ui 1983).

The debris avalanche deposit has a wedge shape, being widest near the volcano and narrowing at greater distances (Figs. 1 and 2) and displays the classic hummocky topography (Fig. 3b) of volcanic avalanches (Ui 1983; Siebert 1984). The avalanche was confined by the sides of the Lauca depression, but climbed ca. 100 m above the valley floor on the southern margins of the depression, more than 200 m above the eastern slope of Guane Guane Hill (12 km west of the source area, Fig. 2), and also more than 30 m near Chucuyo Dome (more than 20 km from the source, Fig. 2).

Field observations

The debris avalanche consists of two units with slightly different distributions, but with marked differences in composition and morphology (Fig. 2). The lower unit is predominantly composed of breccias of flow-banded rhyodacite, glassy dacite, minor fluvial and glacial deposits, pumiceous rhyodacitic block-and-ash flow deposits and large blocks of flow banded rhyodacite, the last two constituents being dominant. The lower unit can be divided into two subunits according to its morphology and granulometry. One subunit consists of large Toreva blocks (Reiche 1937) of rhyodacitic lava domes that crop out in the proximal facies of the avalanche at the western foot of the present volcano (Fig. 2). They correspond to large tilted blocks of the original edifice that slid and came to rest near the volcano. Some Toreva blocks show internal contacts between lava flow units dipping backwards towards the volcano (Fig. 4a). The other subunit is composed mainly of rhyodacitic block-and-ash flow deposits and breccias of flow-banded rhyodacite and minor fluvioglacial deposits. It is buried in many places by the upper unit, outcropping only in the southern and northern margins of the avalanche (Fig. 2). The lower unit shows a smooth undulating morphology with numerous low amplitude hummocks.

The upper unit is composed predominantly of lava, ranging from large coherent blocks to hummocks composed of breccias. The rock types in the upper unit range from basaltic andesite to dacite, with pyroxene andesite and hornblende andesite being dominant. There are numerous, often lake-filled, depressions, tens to hundreds of metres across, in the central and proximal parts of the debris avalanche (Figs. 1 and 4b). In these areas, undisturbed exposures of the lower unit indicate that the upper unit breccia was generally not emplaced in the area of the depression, although, in some of them, there are a few small isolated upper unit hummocks. These depressions are interpreted as large kettle holes, which were originally occupied by large ice blocks when the debris avalanche was first emplaced, which then melted leaving depressions between the hummocks. These blocks came from an ice cap and possible valley glaciers of the old edifice that were incorporated into the avalanche when the collapse took place. Similar but smaller-scale structures were observed and described by Branney and Gilbert (1995) in an eruption-induced lahar deposit from
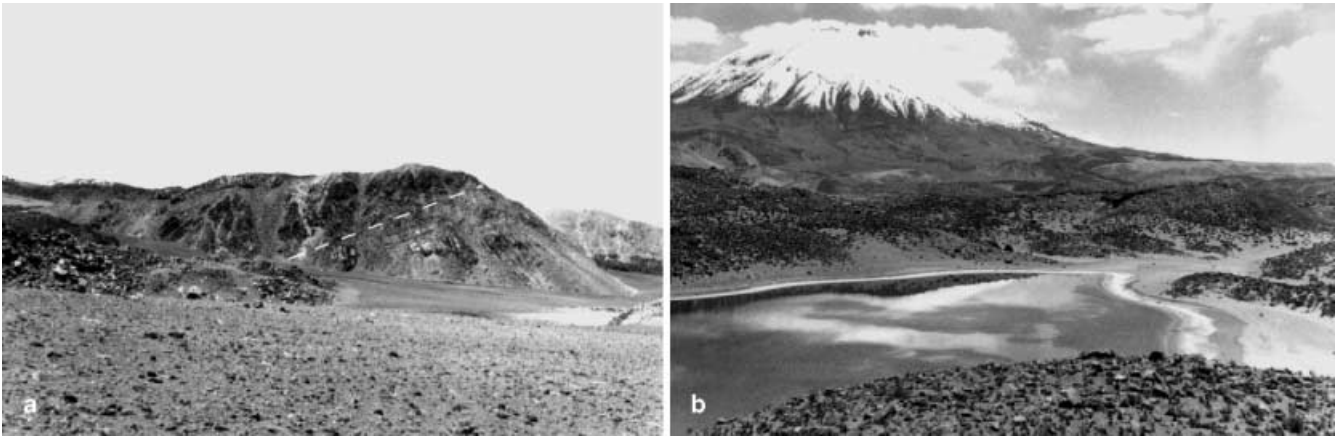
Fig. 4 a Proximal Toreva block (3 km west of Parinacota Volcano) view from north, showing original bedding dipping backwards. Hummock is ca. 100 m high. **b** Kettle hole structure in medial facies of Parinacota avalanche (ca. 8 km from Parinacota Volcano). Lake is ca. 150 m in diameter, surrounded by hummocks of the upper flow unit
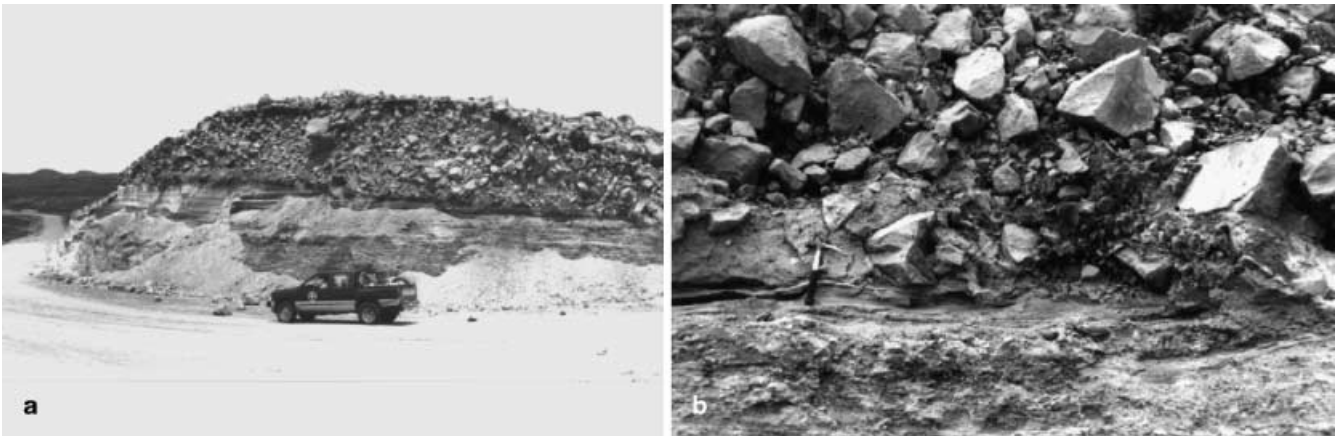

Fig. 5 a Cross section through a hummock near the southern margins of the Parinacota debris avalanche (13 km west of the source, near Parinacota village). Here the upper unit rests directly on lake sediments of the Lauca basin. The hummock is made of a coarse-grained clast-supported breccia, consisting mainly of hornblende andesite. **b** Close-up of the base of the exposure in Fig. 5a showing the fines-poor character of the breccia and angular shape of clasts. Clast surfaces are mixtures of pre-existing fracture faces and new fractures related to fragmentation during emplacement. Note that some fragments are incorporated into the top of the lake sediments. *Hammer* is 30 cm long

Hudson Volcano in southern Chile. Those structures differ from those of Parinacota avalanche in that the ice melting produced collapse pits and ring fractures. There is no evidence of collapse pits nor ring fractures in the Parinacota avalanche deposit, probably because of the coarse character of the deposit and because the ice blocks were big enough not to be buried by the deposit. This study is largely concerned with the features of the upper unit, which buries the lower unit in most places (Fig. 2).

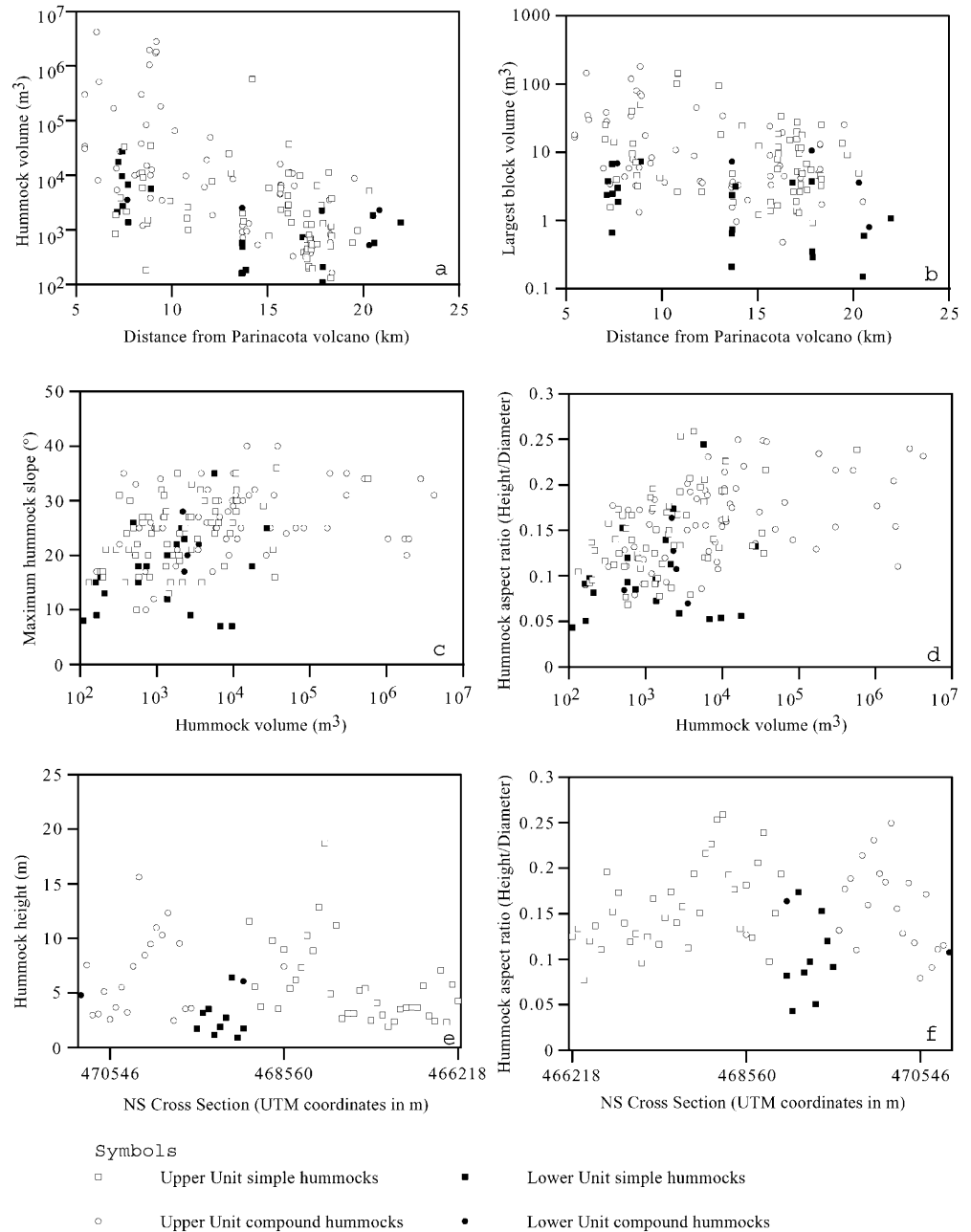The hummocks of the upper avalanche unit are formed of large single blocks or more commonly brecciated lava (Fig. 5a, b). We measured the overall geometry of 150 hummocks from proximal to distal and central to marginal areas of the avalanche deposit. For each hummock, we located the summit and measured the distances and declination from the summit to the edge in four orthogonal directions. For elongated hummocks, two of the directions were along the long axis. From these data we calculated the height of the hummock and average radius using the four distance measurements. We approximated each hummock as an ellipse in plan-form and calculated the volume from the minor and major ellipse axes of the plan-form and from the height. We have considered, for the purpose of volume estimation, compound hummocks (as will be described later) as individual hummocks. We also measured the three orthogonal lengths of the largest block within each hummock, and calculated block volumes assuming an ellipsoidal shape.

There is a general tendency for hummock volumes (ranging from about 1×10^6 m^3 to less than 10 m^3) and the maximum block volume to decrease with distance (Fig. 6a, b). However, at any given distance, there is a wide range of both hummock and maximum block volumes. There is a wide range in the maximum slope angle of the hummocks (Fig. 6c). There is also a tendency for larger hummocks to have higher maximum slopes than

Fig. 6 Geometric features of hummocks from Parinacota avalanche deposit (150 hummocks measured). **a** Hummock volume vs distance from the source. **b** Volume of largest block in hummock vs distance from the source. **c** Maximum angle of hummock slope vs hummock volume. **d** Hummock aspect ratio vs hummock volume. **e** Height variation in a N–S cross section. **f** Aspect ratio variation in a N–S cross section

Symbols

□ Upper Unit simple hummocks   ■ Lower Unit simple hummocks

○ Upper Unit compound hummocks   ● Lower Unit compound hummocks

smaller hummocks (Fig. 6c). Many hummocks have maximum slope angles well below typical angles of static friction for granular materials (26–35°). There is a tendency of the hummock aspect ratio, defined as the hummock height, H, divided by the mean hummock diameter, D, to decrease with decreasing hummock volume (Fig. 6d). In general, hummock size, aspect ratio and maximum slope tend to decrease with distance along the avalanche. A north–south cross section of the hummocks, almost orthogonal to the flow direction, located between 13 and 16 km from the volcano, shows that hummock height and aspect ratio tend to decrease from central areas to flow margins (Fig. 6e, f). It is also clear that hummocks of the lower unit are smaller and have

lower angle slopes than those from the upper unit (Fig. 6a, c, e).

These geometric variations are accompanied by some progressions in the characteristic features of the hummocks. Near the foot of the volcano, Toreva blocks with coherent internal stratigraphy are found with heights of up to 100 m and areas of several hundreds of square metres (Fig. 4a). Other large hummocks in proximal areas can sometimes show coherent internal stratigraphy, such as large blocks (up to several tens of cubic metres) including internal brecciated contacts between different lava flows. Smaller, more distal hummocks usually are only made of brecciated lava with internal structures that are no longer preserved. Asymmetric and elongated

Fig. 7 a Simple conical distal hummock made-up of one lithology breccia (hornblende andesite). Hummock is ca. 25 m high. **b** Compound distal hummock (ca. 16 km from Parinacota Volcano) formed by three individual hummocks (each with different lithologies) amalgamated in one complex hummock. *Numbers* show order of emplacement, view towards direction of flow (*arrow* marks man for scale). **c** Plan view scheme of Fig. 6b compound hummock showing the relationship between the order of deposition and direction of flow

hummocks mainly show two systematic trends of long axes or steepest sides with respect to flow direction. They are usually parallel or orthogonal to the main flow direction, being predominantly parallel to the flow at or near the flow margins.

We have identified two main categories of hummocks with slightly different features. Simple hummocks (Fig. 7a) are those that have relatively simple shapes, commonly conical, and are usually made of only one rock type, which can occur as just one megablock or a pile of breccia. Compound hummocks (Fig. 7b, c) are those that have complex shapes and commonly contain more than one lithology. Commonly, they consist of individual hummocks, each one with its own characteristic lithology. The individual hummocks were amalgamated to each other preferentially along the flow direction. As seen in Fig. 7b, c, the earlier hummock that first came to rest is overlain by two younger hummocks that came to rest on the upstream side of the first hummock to form a more complex shaped compound hummock. These compound hummocks sometimes form ridges up to several hundreds of metres long, especially near and parallel to the margins in the proximal and medial areas. Compound hummocks also occur in the central part of the avalanche deposit where their elongated ridge is usually parallel or orthogonal to the main flow direction.

Two kinds of avalanche margins have been recognised in the deposit. One is very sharp and steep, and tends to develop in proximal and medial areas (Fig. 8a), but it can also occur in distal areas. Typically this kind of margin consists of a linear ridge of coalesced hummocks. Underlying deposits of the lower avalanche unit, fluvial gravels and lacustrine sediments are commonly deformed at the margins with complex folding and faulting
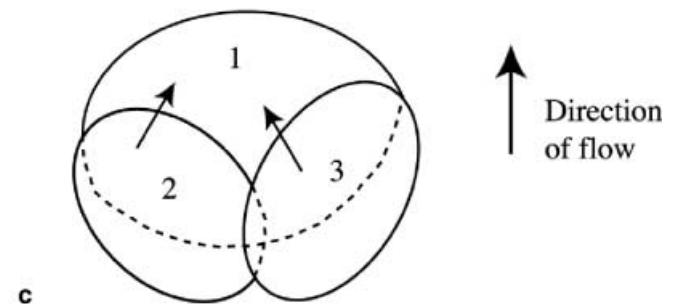
(Fig. 8b). Deformation of the substrate has also been described in other volcanic debris avalanche deposits, where the phenomenon has been named a bulldozer structure (Belousov et al. 1999). Although bulldozer structures are more common in marginal areas and the avalanche front in distal areas, they also occur locally in the central part of the avalanche. The other kind of margin consists of a wedge in which the deposit thins and then merges into a zone of isolated small hummocks and scattered blocks (Fig. 8c, d). A well-defined margin cannot be recognised because the separation of isolated hummocks and scattered blocks increases until there is negligible deposit over distances of tens to hundreds of metres (Fig. 8d). This wedge-type margin characterises more distal areas, covering more than 30 km². Some isolated distal hummocks in the central part of the deposit also show these features. A semicircle of scattered blocks commonly occurs a few metres downstream of isolated hummocks. The scattered blocks are interpreted as the consequence of loose surface blocks that continued their forward motion as the hummock came to rest.

Cross sections through hummocks show that, internally, the breccias of the upper unit are typically clast-supported with almost no fine-grained matrix (particles smaller than 1 cm form less than 1% by volume of the deposit) even in distal facies (Fig. 5a, b). Breccia fragments are always angular, despite the distance from the source area (Fig. 5b). There are no indications of abrasion of the individual clasts. Corners and edges are usu-

Fig. 8 a Steep-sided abrupt flow front on the southern margin of the debris avalanche. Quisiquisini Volcano is seen in the background. Hummock height is about 20 m (*arrow* marks electric post for scale). **b** Small distal hummock (ca. 20 km from Parinacota Volcano) showing deformed and faulted fluvioglacial deposits by the upper ava-lanche breccia. Hammer is 30 cm long. **c** Distal margins of the debris avalanche (near Chucuyo Dome) where the deposit thins to a scatter-ing of blocks on the pre-existing ground made of Upper Tertiary ig-nimbrite. **d** Distal isolated hummocks separated by tens to hundreds of metres from each other (*arrow* indicates man for scale)
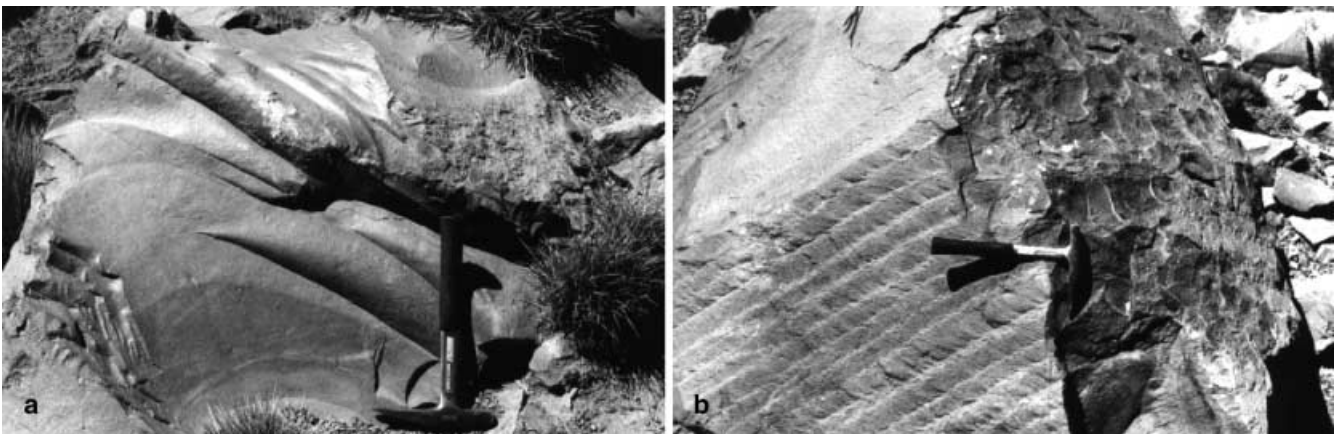

Fig. 9 a Surface of andesite block in debris avalanche showing typical curviplanar and cylindrical thermal fractures formed dur-ing cooling of lava. **b** Surfaces of andesite block in debris ava-lanche showing one face with numerous impact marks and others with thermal fractures and no impact marks

ally sharp and jagged. In most cases, the surfaces of blocks in the breccia are pre-existing thermal fractures and/or weathered joints (Fig. 9a, b), indicating that the rocks in the original stratocone disintegrated preferen-tially along pre-existing weaknesses during avalanche emplacement. However, there are also very angular fresh fracture surfaces in some blocks, particularly in smaller more distal hummocks (Fig. 5b), which indicate that

Fig. 10 a Andesite block showing area affected by multiple impacts with coalescence of shallow dish-shaped impact marks. Note that the left hand side of the flat weathered surface has no impact marks. Hammer is 30 cm long. **b** Detail of surface of andesite block displaying multiple impact marks. Hand lens is 4 cm wide. **c** Surface of andesite block displaying multiple impact marks. Hammer is 30 cm long. **d** A localised narrow zone of impact marks indicates repeated collisions of the same blocks with minor lateral movement. Hammer is 30 cm long

some fragmentation occurred during the final stages of emplacement.

Many blocks show small-scale impact marks, which are particularly well developed on the weathered surfaces of andesite blocks (Fig. 10). An impact mark typically consists of a shallow depression of about 1 to 5 cm in diameter (Fig. 10b) and 0.5 to about 1.5 cm deep in the weathered surface of the rock, and penetrating into fresh unweathered rock. The depression has the shape of a shallow dish. Small concoidal fractures are sub-parallel to the depression margins (Fig. 10a). Complementary thin rock flakes can be found on the avalanche surface. In some cases, block surfaces are covered with tens or even hundreds of impact marks without any systematic pattern (Fig. 10c). In other examples, impact marks are confined locally on the surface (Fig. 10b) and sometimes occur along narrow zones (Fig. 10d). Some blocks have impact marks on all sides, but more commonly one side of a block has large numbers of impact marks whereas the other sides have few marks or none at all (Figs. 9b and 10a).

The base of the debris avalanche is exposed in several areas and is characterised typically by a basal layer of structureless sand and pebbles. This basal deposit almost always separates both the upper and lower avalanche units from the ground. Its thickness varies from a few centimetres to over a metre and can fluctuate significantly over distances of only a few metres. In some exposures, the lower unit is missing and the basal layer forms a matrix between lava fragments at the base of the upper unit. The lithology of the components in the basal layer deposit is identical to the pebbles and sand in the sandy conglomerate facies of the Lauca basin sediments. The only difference is that primary sedimentary structures are no longer preserved.

Two kinds of contact have been observed between the basal layer and the substrate. Where the avalanche overlies welded tertiary ignimbrite there is no disturbance of the ground. However, where the avalanche overlies Lauca basin sediments, complex deformation structures are observed. Pieces of sediment are rafted within the basal deposit. The sedimentary layers of the Lauca sediments commonly display boudinage, folding and faulting with thrust structures being common. In some exposures the basal layer deposits are mixed in a complex way with the underlying sediments.

Discussion

The geological observations of the Parinacota debris avalanche place some important constraints on the mechanisms of transport and emplacement of debris avalanches. The avalanche is attributed to the failure of a large volcanic edifice constructed over a sedimentary basin filled with lacustrine, fluvial, glacial and pyroclastic deposits. There was also significant ice and perhaps snow present, probably as an ice-cap to the stratocone and valley glaciers. Loading deformation, sometimes with eventual edifice sector collapse, have been documented elsewhere (Merle and Borgia 1996; Van Wyk de Vries and Borgia 1996; Van Wyk de Vries and Francis 1997). Strong deformation of these basin sediments and pyroclastics indicates that an important part of the upper Lauca basin to the west of Parinacota Volcano was occupied by a lake. The ancestral volcanic edifice failed sequentially to produce a lower avalanche unit derived from the rhyodacitic lower parts of the edifice, and an upper avalanche unit derived from the predominantly andesitic upper parts of the edifice. Where the avalanche base is exposed there is always a basal layer (typically less than 1 m thick) of structureless pebbly sand, which is attributed to shearing of coarse-grained fluvial deposits as the avalanche advanced across the basin. This basal layer of sedimentary material is thought to have accommodated much of the shear needed for the avalanche to flow. A similar basal layer, of different origin, has also been observed in other debris avalanche deposits (Belousov et al. 1999).

We now focus on the coarse-grained upper avalanche unit. The most prominent feature of the upper avalanche deposit is its very coarse grain size, with no fine matrix (fragments smaller than 1 cm form less than 1% by volume of the deposit). The blocks in the breccia are characteristically angular with sharp edges and corners. Thus, there is no evidence of significant abrasive rounding. At least within the interior of hummocks, the avalanche cannot be the result of agitated granular flow mechanisms (Drake 1990; Straub 1996; Iverson 1997) in which there are strong interactions between particles, including rotations, numerous collisions, sliding and local mixing. Most of the rock fragments of the avalanche deposits are mostly bounded by weathered or thermal fracture surfaces that must have existed in the edifice before the collapse. Thus, much of the character of the deposit reflects the distribution of fractures and weaknesses in the edifice prior to collapse that are observed in older Parinacota domes and lava flows not involved in the collapse. The edifice disintegrated during the failure to form the breccia. Some rock clasts, however, have relatively freshly-formed surfaces because of some break-up during avalanche emplacement.

The occurrence of the impact marks shows that there were localised collisions between neighbouring blocks and projectiles. There is no evidence of rapid sliding with strong frictional contacts, as has been inferred from the friction marks with slickensided surfaces observed on blocks from pyroclastic flow deposits of the Soufrière

Hills volcano, Montserrat (Grunewald et al. 2000). The common occurrence of many impact marks in localised areas (some of them defining narrow trends of impacts) suggests that some neighbouring blocks were vibrating and repeatedly colliding, but without significant shearing motion relative to one another. However, minor flow differential motion is implied by the occurrence of narrow zones of localised impact marks. We observed most impact marks at the surfaces of hummocks. Therefore, some impact marks may have been caused by freely moving projectiles in the overlying avalanche immediately after deposition of a hummock. The occurrence of free projectiles in the upper part of the moving avalanche has also been suggested for the Jocotitlán avalanche (Siebe et al. 1992), but these authors have not described the presence of impact marks in that deposit. Melosh (1979) has proposed the idea of acoustic fluidisation in which vibrations reduce the strength of debris. Although our observations support the idea of vibrational interactions, the very coarse-grained character of the Parinacota avalanche does not favour a fluidisation mechanism. Melosh (1979) also proposed that vibrations lowered the friction of the rock mass enabling easier flow, but observations at Parinacota avalanche deposit do not support internal flow within the domains during transport.

We have applied ideas on the impact of projectiles onto rock surfaces to estimate flow conditions. Consider a locally spherical portion of rock with radius r impacting a plane rock surface at normal velocity V. The impact could be the result of either two large rocks colliding with a protrusion of the first impacting onto the second or by a fast-moving projectile hitting the rock surface. The rock surface is compressed at first elastically and then plastically to lead to lateral spall cracks emanating from the base of the damage zone, as described in Lawn (1993). Extending the concepts laid out there to this somewhat different situation, we consider a protrusion that penetrates into the rock a distance h. This will lead to a roughly hemispherical damage zone of radius a. By use of Pythagoras' theorem for $h<<r$, or by geometry, it is straightforward to show that $h=0.5a^2/r$. The force, F, of the impact is distributed over the damage zone to lead to a contact pressure, ρ_0, which is known as the hardness of the material and is related to F by $F=\pi a^2\rho_0$. During the collision the kinetic energy of the impacting rock, $E=1/2\ MV^2$, where M is the mass of the rock, is transformed into plastic strain energy, P, which is stored in the damaged rock. In terms of the quantities already defined, P is given by

$$P = \int_0^z F\,dz = \pi\rho_0 \int_0^z a^2\,dz = 2\pi\rho_0 \int_0^z z\,dz$$

$$= \pi r\rho_0 z^2 = \frac{1}{4}\pi\rho_0 a^4/r \tag{1}$$

Equating E to P, we obtain:

$$V = \left(\frac{1}{2}\pi\rho_0/Mr\right)^{1/2} a^2 \tag{2}$$

Assuming a typical value of $\rho_0 = 2 \times 10^9$ Pa, $M = 10^3$ kg, $r = 0.02$ m and $a = 0.01$ m, we obtain $V = 1.3$ m s^{-1}. Thus, the impact marks can be generated by movements that are a small fraction of the expected typical velocity of the avalanche. In this case, the avalanche velocity can be estimated as at least 60 m s^{-1} when it reached the Guane Guane Hill and ca. 25 m s^{-1} near Chucuyo (12 and 20 km from the source, respectively) by using $v = (2\,gH)^{1/2}$, with H being the run-up.

The hummocky topography provides further constraints on emplacement mechanisms. There are general progressions of hummock size, shape and internal organisation from proximal to distal areas and towards the flow margins. In proximal areas many larger hummocks are composed of shattered rock, but with internal stratigraphy derived from the original edifice preserved. Such hummocks form a continuum, with Toreva blocks that lack internal disruption. Smaller hummocks and those further from the source are internally fragmented into a chaotic breccia, although remnant stratigraphy can sometimes be discerned. Taken together with the absence of abrasive rounding of the breccia blocks, we surmise that each hummock represents a domain of rock within the edifice. We propose that when the edifice failed it disintegrated preferentially along pre-existing fractures and planes of weakness into a wide range of domains and that there was further break-up into smaller domains during emplacement and spreading of the avalanche. The general decrease of hummock size with distance and the wide range of hummock sizes deposited at any given distance (Fig. 5a) can be explained by an interplay of three factors. First, the edifice broke up initially into a wide range of domain sizes. Second, there was further break up of the rock mass during emplacement so that size decreased with residence time in the avalanche and therefore distance. Third, there were variations of strength of the rocks composing the domains such that weaker regions broke up more than stronger regions. The role of rock strength is also indicated by the observation that the amplitude and size of hummocks composed of block-and-ash flow deposits in the lower avalanche unit are both smaller than most of the lava hummocks in the upper avalanche unit (see Fig. 6a, c, e).

Many of the hummocks have maximum slope angles well below the expected angle of repose of granular materials (>25°). Thus their shapes cannot be attributed simply to adjustments of the hummock margins after emplacement to a static equilibrium. Rather we postulate that the low maximum slope angles of many hummocks are governed by dynamic processes related to emplacement. In distal areas, cross sections through low-amplitude hummocks show blocks with fresh fractures surfaces as well as pre-existing fracture surfaces. Two mechanisms may have contributed to the formation of low amplitude hummocks, well below the angle of repose of granular material. First, the domains that travelled furthest may have been deposited with higher kinetic energy and have spread out dynamically as they were deposited. Second, the avalanche spread out as it was emplaced with much of the deformation accommodated on the basal layer. Thus, a mechanism of reducing the hummock slope angle and amplitude is by spreading of the underlying basal layer, as has been shown experimentally (Merle and Borgia 1996). Coupling of the overlying breccia domains with the basal layer would result in spreading of a hummock.

Where exposed, the base of the debris avalanche deposit consists of a structureless sedimentary layer. The very coarse character of the whole deposit, with the exception of this structureless basal layer, and the absence of any fluidisation structure make very unlikely that factors, such as the presence of a pressurised air layer (Shreve 1968) or "self lubrication" (Campbell 1989), could explain the transport and long run-out of the Parinacota avalanche. The presence of a fine-grained basal layer, as has been observed in other debris avalanche deposits (Belousov et al. 1999), can explain where most of the shearing and deformation was accommodated during emplacement.

Here we emphasise that this debris avalanche essentially involved the deformation of a conical-shaped rock mass (the volcanic edifice) into a thin sheet (the avalanche deposit) in a fluid-like manner. Thus, deformation within the basal layer alone cannot explain the overall spreading of the whole body of the flow. Also, because spreading does occur and because of the sedimentary origin of the basal layer it is suggested that Bingham flow (Eppler et al. 1987; McEwen and Malin 1989) or plug-flow models (Takarada et al. 1999) are not appropriate to explain its transport. The absence of any basal melted layer, as has been observed in other debris avalanches (Goguel 1978; Erismann 1979; Legros et al. 2000), suggests that frictional heating was unimportant. Indeed, the overall spreading of the avalanche above the basal layer requires extension of the domains. We envisage that there is negligible frictional resistance between the domains to extension. Some compression, however, is locally evident at the flow margins, where hummocks are oriented parallel to the flow margins, and also by the occurrence of bulldozer structures.

The role of water in the transport of long run-out debris avalanches is still controversial. Crandell et al. (1984) and Crandell (1989) have suggested that the incorporation of water-rich sediments into the matrix of the ancestral Mount Shasta debris avalanche could have helped give it its great mobility, whereas Siebe et al. (1992) suggested a similar 'helping' mechanism to explain the long run-out of the Jocotitlán avalanche in Mexico. On the other hand, McEwen (1989) deduced that Valles Marineris avalanches on Mars were dry, whereas Stoopes and Sheridan (1992) have suggested that the role of water in the transport mechanism of the Colima debris avalanche, Mexico, was irrelevant. In the case of the Parinacota debris avalanche, the basal sediment shear layer is likely to have had a high water content. The upper part of the Lauca basin (where the avalanche was deposited) was partially occupied by a lake and wet lacustrine sediments. Water incorporated into

the base could also have aided avalanche transport by reducing the basal frictional resistance. The occurrence of large kettle hole structures indicates that a significant amount of ice and snow was involved in the collapse and was incorporated into the avalanche. As was the case in the 1980 debris avalanche of Mount St Helens (Glicken 1996), melting of large ice blocks would have been negligible during the time-scale of avalanche emplacement. On the other hand, significant amounts of ice and snow might help explain the enigmatic origin of the wedge-shaped distal margins where the deposit becomes discontinuous with isolated hummocks and scattered blocks in between. If the distal avalanche had either contained or incorporated ice and snow that subsequently melted (as is suggested by the presence of kettle hole structures in more proximal areas), then the discontinuous character of the margins could result. This interpretation is also consistent with the origin of small isolated hummocks in the depressions of kettle holes, where there is good evidence that the avalanche deposit consisted largely of ice.

Synopsis of the model for Parinacota avalanche emplacement

We interpret the features of the debris avalanche deposit in terms of the concept of domains. The original stratocone was probably comparable in volume to the Holocene cone, and largely made of lava with subsidiary flow margin breccias built above a series of rhyodacitic domes and their related pyroclastic flow deposits. This edifice was partially constructed on top of fluvial and lacustrine sediments. From the occurrence of kettle holes and the post-glacial age of the deposit we also surmise that there was an ice cap, valley glaciers, shallow lakes and wet soft sediments present in the area. The debris avalanche is divided into two units. The lower unit is predominantly composed of pyroclastic deposits and subsidiary fluvial, glacial and lacustrine sediments of the Lauca basin. We suggest that the dense edifice loaded the lower density sediments. Failure of the relatively weak sedimentary lithologies beneath and adjacent to the stratocone caused the edifice to collapse to form the avalanche. The failure could have been triggered by a regional earthquake or because of magmatic activity, but there is no direct evidence yet of either mechanism. However, loading of low-density sedimentary and pyroclastic basin-fill sequences by a dense andesite stratocone is likely to have been the major causative factor in sector collapse.

When the failure took place the volcanic edifice disintegrated preferentially along pre-existing fractures and planes of weakness into large-scale coherent domains of rock with volumes ranging from less than 10 to over 1×10^6 m^3. We propose that each domain on deposition formed a hummock and that separation of the domains by original weaknesses in the edifice allowed the disintegrating volcano to spread in a fluid-like manner to form the debris avalanche. The concept of domains can explain the limited internal deformation within individual hummocks, preservation of internal stratigraphy in some hummocks and the lack of abrasive rounding of blocks in the breccias.

The origin of the hummocks is explained by deposition of these domains. As the front of the avalanche advances, domains will impact the ground. We propose that it is at this late stage that the domains deposit as hummocks. Some of the fragmentation of a domain may occur during transport, with perhaps vibrations contributing to disintegration. The general changes in hummock volumes, aspect ratios and internal features can be accounted for by postulating that material that travels further has broken up into smaller domains because of longer residence time in the avalanche that forms smaller and lower amplitude hummocks. Domains that travel further may also have original higher velocities. The spreading of the avalanche predominantly on its basal layer may cause the overlying breccia domains to spread. Near the source, the domains are generally large and had very low energy. Thus, some do not disintegrate on deposition, resulting in Toreva blocks and large steep-sided hummocks. Thus, the occurrence of smaller and lower amplitude hummocks in more distal areas is a combined effect of both the presence of smaller domains, which were originally more fragmented and travelled further as they had higher velocities, and the result of some fragmentation of bigger domains during transportation of the debris.

The hypothesis of progressive break up of the rock mass and the higher initial kinetic energy of rock mass domains with distance can also explain the difference between proximal and distal flow margins. Near the source, the debris avalanche has sufficient coherence that its margins stop abruptly to form a well-defined flow margin. In more distal localities, the rock mass has disintegrated to such an extent that the small-scale, high energy domains spread out and thin, and even separate from one another, with the formation of isolated small hummocks and rock spray across the ground. The original presence of ice and snow, which subsequently melted, might also contribute to the discontinuous character of these thin margins.

The concept of rock domains may also help to explain the low frictional resistance of debris avalanches (Dade and Huppert 1998). The deformation of the spreading avalanche is accommodated along pre-existing weaknesses, which define the domain volumes, and thus the resisting strength is low. We envisage the rock mass of the edifice dilating as the loading stresses in the edifice are relieved during failure. The basal layer itself, which accommodated much of the deformation, is formed of loose unconsolidated wet sediments, which are expected to have low frictional resistance.

Conclusions

In this study we describe the morphological and textural features of the Holocene Parinacota debris avalanche de-

posit. Key features of this deposit include (1) pronounced hummocky topography, (2) a basal layer of structureless sedimentary material incorporated during run-out from the underlying Lauca basin sediments, (3) the lack of fine-grained matrix in the avalanche deposit, which is otherwise a predominantly andesite-rich, coarse-grained and angular breccia, and (4) ubiquitous, small-scale impact structures on the surfaces of some of the breccia blocks. Additionally we note that (1) the volumes and height to width ratios of individual hummocks tend to decrease with transport distance, (2) the basal sedimentary layer apparently accommodated much of the shear that occurred during emplacement of the spreading avalanche rock mass, and (3) the impact marks occur most prominently on weathered surfaces of large andesite blocks.

These observations on the Parinacota avalanche deposit show that several of the emplacement mechanisms commonly invoked to explain the mobility of large rock avalanches either are inconsistent with the data or fail to explain its major features. The upper unit contains negligible fine matrix, so the role of lubrication by or fluidisation of fines cannot be invoked in the deformation and mobility of the main rock mass. The existence of a pressurised air cushion at the base also seems improbable given the high permeability of the fines-poor breccia and thinness of the deposit in distal areas. Likewise, the absence of abrasive rounding and surface shear features on blocks in the breccia suggest that component particles were not in prolonged shearing contact during transport. Thus, the avalanche mass was not subject to pervasively sheared granular flow. Instead, the impact marks, described here for the first time, record the fact that some clasts were subject to intense vibration, but little relative shear. Overall, the impact marks are interpreted to be the result of repeated collision of neighbouring blocks and perhaps the existence of free rock projectiles. Nevertheless, the debris avalanche has involved the collapse, disintegration and fluid-like spreading of an originally conical rock mass into a thin and very extensive debris avalanche sheet. The main deformation of the spreading avalanche is attributed to the deformation of probably wet sedimentary material at the base of the edifice. The basal layer of sheared sediments probably originated as a décollement surface and accommodated most of the shearing and deformation needed for the avalanche to flow.

We propose that the avalanche resulted from the sector collapse of an ancestral stratovolcano built on top of a lake basin. Upon mobilisation, the edifice disintegrated preferentially along pre-existing fractures and planes of weaknesses, breaking up the rock mass into domains, mainly at early stages when the avalanche first impacted the ground, with some break up occurring during transport and emplacement. The combination of break up into smaller domains as the avalanche spread and higher energies of domains that reached more distal areas resulted in the characteristic hummocky topography, with the decrease in hummock size and amplitude with distance.

References

Belousov A, Belousova M, Voight B (1999) Multiple edifice failures, debris avalanches and associated eruptions in the Holocene history of Shiveluch volcano, Kamchatka, Russia. Bull Volcanol 61:324–342

Branney M, Gilbert J (1995) Ice-melt collapse pits and associated features in the 1991 lahar deposits of Volcán Hudson, Chile: criteria to distinguish eruption-induced glacier melt. Bull Volcanol 57:293–302

Campbell C (1989) Self-lubrication for long run-out landslides. J Geol 97(6):653–665

Crandell D (1989) Gigantic debris avalanche of Pleistocene age from ancestral Mount Shasta Volcano, California, and debris-avalanche hazard zonation. US Geol Surv Bull 1861:1–32

Crandell D, Miller C, Glicken H, Christiansen R, Newhall C (1984) Catastrophic debris avalanche from ancestral Mount Shasta Volcano, California. Geology 12:143–146

Dade W, Huppert HE (1998) Long run-out rockfalls. Geology 26:803–806

Drake T (1990) Structural features in granular flows. J Geophys Res 95(B6):8681–8696

Eppler DB, Fink J, Fletcher R (1987) Rheological properties of the Chaos Jumbles rock fall avalanche, Lassen Volcanic National Park, California. J Geophys Res 92:3623–3633

Erismann TH (1979) Mechanisms of large landslides. Rocks Mech 12:15–46

Francis PW (1993) Volcanoes: a planetary perspective. Oxford University Press, Oxford, pp 1–443

Francis PW, Wells G (1988) Landsat thematic mapper observations of debris avalanche deposits in the Central Andes. Bull Volcanol 50:258–278

Glicken H (1996) Rockslide-debris avalanche of May 18, 1980, Mount St Helens, Washington. USGS Open File Rep 96-677

Goguel J (1978) Scale-dependent rockslide mechanisms, with emphasis on the role of pore fluid vaporisation. In: Voight B (ed) Rockslides and avalanches, vol 1. Natural phenomena. Elsevier, Amsterdam, pp 693–705

Grunewald U, Sparks RSJ, Kearns S, Komorovski JC (2000) Friction marks on blocks from pyroclastic flows at the Soufrière Hills Volcano, Montserrat: implications for flow mechanisms. Geology 28:827–830

Hsü K (1975) Catastrophic debris streams (sturzstroms) generated by rockfalls. Geol Soc Am Bull 86:128–140

Iverson RM (1997) The physics of debris flows. Rev Geophys 35:245–296

Katsui Y, González O (1968) Geology of the neovolcanic area of Nevados de Payachata (in Spanish). Geology Department, Publication no 29, University of Chile

Kött A, Gaupp R, Wörner, G (1995) Miocene to Recent history of the Western Altiplano in Northern Chile revealed by lacustrine sediments of the Lauca Basin (18°15′–18°40′S/ 69°30′–69°05′W). Geol Rundsch 84:770–780

Lawn B (1993) Fracture of brittle solids, 2nd edn. Cambridge University Press, Cambridge

Legros F, Cantagrel JM, Devouard B (2000) Pseudotachylyte at the base of a volcanic landslide deposit: implications for emplacement mechanisms. Abstracts International Association of

Volcanology and Chemistry of the Earth's Interior General Assembly, Bali, Indonesia

McEwen A (1989) Mobility of large rock avalanches: evidence from Valles Marineris, Mars. Geology 17:1111–1114

McEwen A, Malin M (1989) Dynamics of Mount St. Helens' 1980 pyroclastic flows, rockslide-avalanche, lahars, and blast. J Volcanol Geotherm Res 37:205–231

Melosh HJ (1979) Acoustic fluidisation: a new geological process? J Geophys Res 84:7513–7520

Melosh HJ (1987) The mechanics of large rock avalanches. In: Costa JE, Wieczorek GF (eds) Debris flows/avalanches: process, recognition and mitigation. Geol Soc Am Rev Eng Geol 7:41–49

Merle O, Borgia A (1996) Scaled experiments of volcanic spreading. J Geophys Res 101:13805–13817

Reiche P (1937) The Toreva block – a distinctive landslide type. J Geol 45:538–548

Shreve RL (1968) The Blackhawk landslide. Geol Soc Am Spec Pap 108:1–47

Siebe C, Komorowski JC, Sheridan M (1992) Morphology and emplacement of an unusual debris-avalanche deposit at Jocotitlán, central Mexico. Bull Volcanol 54:573–589

Siebert L (1984) Large volcanic debris avalanches: characteristics of source areas, deposits, and associated eruptions. J Volcanol Geotherm Res 22:163–197

Stoopes G, Sheridan M (1992) Giant debris avalanches from the Colima Volcanic Complex, Mexico: implications for long-run-out landslides (>100 km) and hazard assessment. Geology 20:299–302

Straub (1996) Self-organisation in the rapid flow of granular material: evidence for a major flow mechanism. Geol Rundsch 86:85–91

Takarada S, Ui T, Yamamoto Y (1999) Depositional features and transportation mechanism of valley-filling Iwasegawa and Kaida debris avalanches, Japan. Bull Volcanol 60:508–522

Ui T (1983) Volcanic dry avalanche deposits: identifications and comparison with nonvolcanic debris stream deposits. J Volcanol Geotherm Res 18:135–150

Van Wyk de Vries B, Borgia A (1996) The role of basement in volcano deformation. In: Mcguire WJ, Jones AP, Neuberg J (eds) Volcano instability on the earth and other Planets. Geol Soc Spec Publ 110:95–110

Van Wyk de Vries B, Francis P (1997) Catastrophic collapse at stratovolcanoes induced by gradual volcano spreading. Nature 387:387–390

Wörner G, Harmon R, Davidson J, Moorbath S, Turner D, McMillan N, Nye C, López L (1988) The Nevados de Payachata volcanic region (18°S/69°W, N Chile). 1. Geological, geochemical, and isotopic observations. Bull Volcanol 50:287–303

Wörner G, Hammerschmidt K, Henjes-Kunst F, Lezaun J, Wilke H (2000) Geochronology (40Ar/39Ar, K–Ar and He-exposure ages) of Cenozoic magmatic rocks from northern Chile (18–22°S): implications for magmatism and tectonic evolution of the central Andes. Rev Geol Chile 27(2):205–240